Available online at www.sciencedirect.com
ScienceDirect
Chinese Journal of Aeronautics 21(2008) 506-511
Chinese Journal of Aeronautics
www.elsevier.com/locate/cja

Influences of Geometric Parameters upon Nozzle Performances in Scramjets

Li Jianping*, Song Wenyan, Xing Ying, Luo Feiteng

School of Power and Energy, Northwestern Polytechnical University, Xi'an 710072, China

Received 21 November 2007; accepted 27 April 2008

Abstract

This article investigates and presents the influences of geometric parameters of a scramjet exerting upon its nozzle performances. These parameters include divergent angles, total lengths, height ratios, cowl lengths, and cowl angles. The flow field within the scramjet nozzle is simulated numerically by using the CFD software—FLUENT in association with coupled implicit solver and an RNG k-ε turbulence model.

Keywords: scramjet; nozzle; numerical simulation; geometric parameters

Nomenclature:

C_T— thrust coefficient; C_N— lift coefficient
C_M— pitching moment coefficient
L— nozzle total length; T— nozzle thrust
N— nozzle lift; M— nozzle pitching moment
L_V— the length of vehicle
β_B— divergent angle; H_2/H_1— height ratio
θ — nozzle cowl angle; L_s— cowl length

1 Introduction

A scramjet generally consists of an inlet, an isolator, a combustor and a nozzle. As an important component, the nozzle produces most of thrust, whose magnitude and direction have decisive effects on the scramjet performances. Therefore, the research on nozzles has long been attracting rapt attention with the focus on the effects of geometric parameters upon their performances. In NASA, the Langley center, having this subject as its key object of scramjet research, designed a scramjet nozzle of fixed geometry[1] and found that, the nozzle would generate maximum thrust with the minimum divergent angle when the angle of attack was zero. When the angle of attack was 8°, the thrust depended on the obliquity of nozzle top-wall and when the obliquity reached 19.8°, the nozzle produced the maximum thrust. The effects of cowl length on the thrust and the balance of aircraft was also investigated with the conclusion that the performances will be ameliorated when $L_s = 3.12H_1$. A shorter cowl length can result in decreased thrusts, overmuch lifts and nose- down pitching moments due to decreased top-wall pressure caused by non-uniform expansion. On the contrary, a longer one could cause additional nose- up pitching moments. However, up to now few works have been published about the dependence of scramjet nozzle performances upon the geometric parameters. This article is intended to make an insight into the influences of divergent angles, total lengths, height ratios, cowl lengths and cowl angles upon scramjet nozzle performances by way of numerical simulation, and presents the detailed data thereon.

2 Experimental Verification of Calculated Results

In order to verify the feasibility of numerical

*Corresponding author. Tel.: +86-29-88494852.
E-mail address: lijianping001@mail.nwpu.edu.cn

results by using FLUENT software, this article takes Japan NAL—KRC's scramjet nozzle test[2] as an example. When the gas flows into the scramjet nozzle, it would be continuously in the state of chemical reaction because of inadequate combustion. Sangiovanni, et al.[3] studied the effects of hydrogen/air chemical reaction on scramjet performances and found that the gas chemical reaction in nozzle, even though intensive and strong, made little contribution to the specific impulse and thrust of scramjet. Therefore, the gas flow in the nozzle could be considered as a reaction-freezing flow in numerical simulation. Thus the inflow of the nozzle under study is viewed as reaction-freezing, and the specific heat ratio is set to be 1.33. The condition for calculation contains coupled implicit solver, adaptive structured grid and RNG k-ε viscous model, which can provide an analytical expression by taking into account the viscosity in the low Reynold number flow to perform a better simulation in the laminar flow region near the walls, thus achieving a high accuracy and creditability of simulation in a wider range.

Free-stream parameters are $T^* = 673$ K, $p = 2\,940$ Pa, $Ma = 7.1$; Nozzle inflow parameters are $T^* = 300$ K; relative static pressure $p_{inc}/p_\infty = 1.58$, $Ma = 2.5$; Atmospheric pressure is $p_\infty = 2\,940$ Pa .

The data obtained from the test are about the static pressure distribution of nozzle top-wall centerline. Both numerical and experimental results are non-dimensionalized by the plenum chamber pressure p_{pc}. As seen from Fig.1, a good agreement is achieved between calculated and experimental results in both changing trend and numerical values.

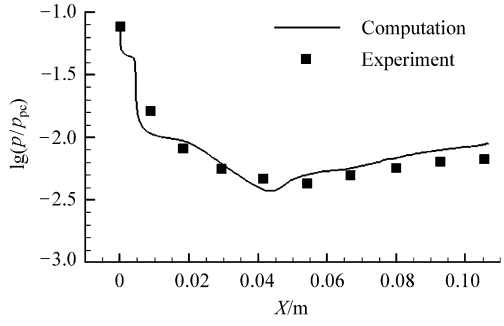

Fig.1 Pressure distribution on nozzle top wall.

3 Research on Scramjet Nozzle Performances

Let the entrance point at the nozzle bottom-wall be the Cartesian coordinate origin, the center-of-mass coordinate be $(-12.5H_1, 0)$ according to Ref.[4], the length of vehicle $L_V = 75H_1$, the height of inlet $5.33H_1$, the width of inlet 1 m, and then the maximal capture area of inlet from calculation $A = 5.33H_1 \times 1$ m$= 0.16$ m^2.

At the designed point, assume the flight height $H = 25$ km and the flight Mach number $Ma = 6$.

The inflow parameters of the nozzle can be obtained from 1D calculation of combustor. The given inflow conditions are: Mach number $Ma_1 = 1.59$, static temperature $T = 1\,622.21$ K, static pressure $p = 73\,660.91$ Pa, height $H_1 = 0.03$ m; divergent angle β_B are initiated. This article uses the maximal thrust method[5] to design various nozzle contours with different geometric parameters and the FLUENT 6.0 to perform the numerical simulation of the nozzle flow field and performances. Fig.2 shows the computational domain. The simulation conditions for FLUENT 6.0 are the same as cited before. The nozzle inflow parameters are assumed the same as in designed state with the nozzle outflow pressure being 2 000 Pa. Moreover, the nozzle wall is assumed adiabatic and non-slip.

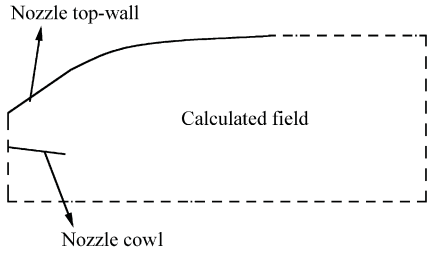

Fig.2 Calculated field.

3.1 Influences of divergent angle upon nozzle performances

Fig.3 shows various nozzle top-wall contours with different β_B. In it, $L_s = 3.12H_1$, $\theta = 0°$ with a constant. nozzle total length at $L = 25H_1$. As H_2/H_1 varies with β_B slightly, its influences can be ignored. Fig.4 shows the variation of C_T, C_N, and C_M with β_B.

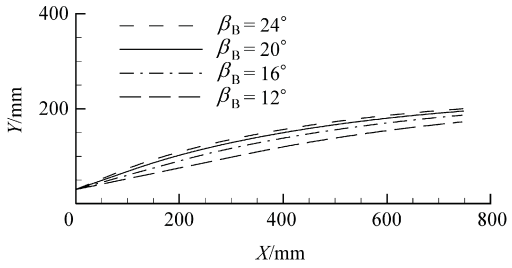

Fig.3 Top wall contours with different β_B.

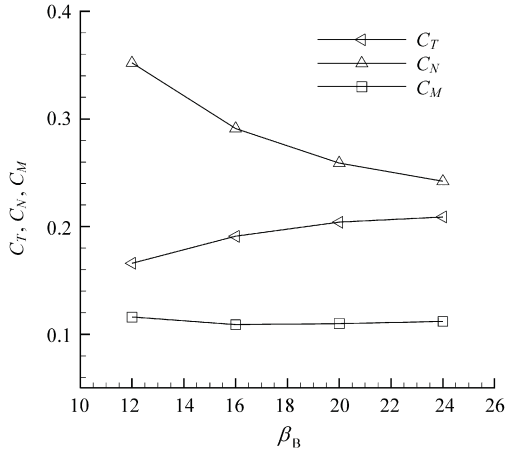

Fig.4 Variation of C_T, C_N, and C_M with β_B.

The calculated results indicate that, the variation of thrust coefficient C_T with the divergent angle β_B tends to increase while it decreases with the lift coefficient C_N, and nothing significant of the pitching moment coefficient C_M. This might be attributed to the dependence of magnitude of thrust on the top-wall pressure and the divergent angle. With divergent angle increasing, the X-component of top-wall pressure and thrust increase, thus making C_T increase simultaneously and the Y-component of top-wall pressure decreases with some reduction in the negative lift, thereby decreasing C_N. When the divergent angle increases, the nozzle thrust and lift tend to vary in opposite direction with each changing value approaching the same, making C_M vary slightly due to the combined effects of T and N.

Moreover, the sensibility of C_T to β_B is analyzed through the following definition:

$$K = \left| \frac{\text{variation of dependent variable(for example,}\Delta C_T\text{)}}{\text{variation of independent variable(for example,}\Delta\beta_B\text{)}} \right|$$

From the above-cited discussion, it is clear that C_T, C_N, and C_M would be more sensible, the higher the K-value is. The calculated results show the sensibility coefficients of C_T, C_N, and C_M to β_B being 0.26, 0.31 and 0.04 respectively，when β_B falls in the interval between 12° and 24°. In terms of their sensibility to β_B, C_T, C_N, and C_M change in an escalating order. Therefore, the effects of β_B on C_T, C_N, and C_M should be taken into synthetic consideration when choosing the value of β_B.

3.2 Influences of nozzle total length upon nozzle performances

In Fig.5, which shows various nozzle top-wall contours with different L, four different contours can be obtained by truncating between the points of $L = 15H_1$, $L = 20H_1$, $L = 25H_1$, and $L = 30H_1$. Under the constant geometric condition: $\beta_B = 20°$, $L_s = 3.12H_1$, and $\theta = 0°$, when the value of L decreases from $30H_1$ to $15H_1$, H_2/H_1 varies as little as no more than 1.6, meaning its influences could be ignored. The changes of C_T, C_N, and C_M with L are shown in Fig.6, which indicates that all C_T, C_N, and C_M decrease as L decreases, though the variation of C_T appears less distinct. The calculated results also show that when L decreases from $30H_1$ to $15H_1$, C_T,

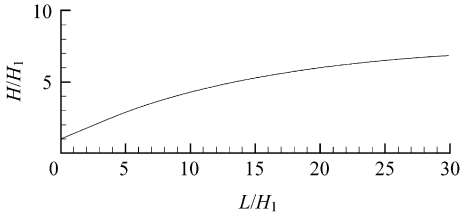

Fig.5 Top-wall contours with different L.

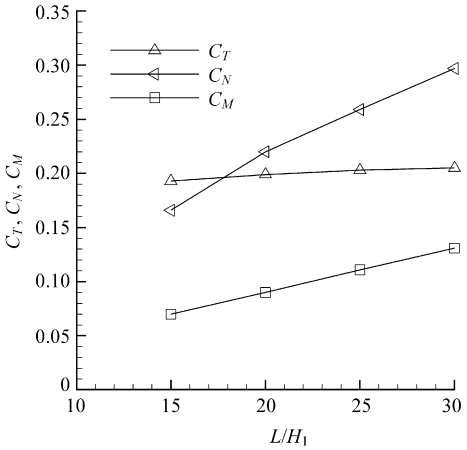

Fig.6 Variation of C_T, C_N, and C_M with L.

C_N, and C_M drop by 5.9%, 44.2%, and 46.4% while the sensibility coefficients of C_T, C_N, and C_M to L are 0.12, 0.88 and 0.92 respectively. It is clear that in terms of sensitivity to L, C_T, C_N, and C_M come in a descending order. Therefore, on the premise of escalating sufficient nozzle performances, a less total length is more preferable in the nozzle design if taking into account the weight constraint.

3.3 Influences of height ratio H_2/H_1 upon nozzle performances

Fig.7 shows nozzle top-wall contours with different H_2/H_1, given $L = 25H_1$, $\beta_B = 20°$, $L_s = 3.12H_1$, and $\theta = 0°$.

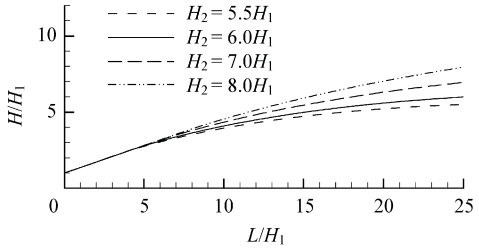

Fig.7 Top-wall contours with different H_2/H_1.

The variations of C_T, C_N, and C_M with H_2/H_1 are shown in Fig. 8, which indicates that the pressure of internal nozzle varies slightly with H_2/H_1 because of the same expansion degree of internal nozzle with the invariable β_B, and the pressure of external nozzle declines slowly along X-axis at a small H_2/H_1, but sharply at a large one because the higher expansion degree of external nozzle makes the top-wall pressure drop rapidly along X-axis.

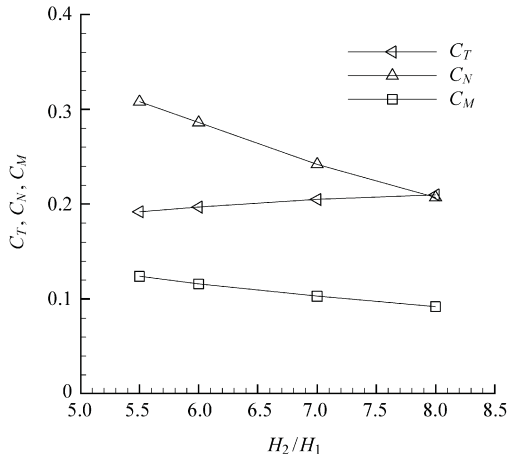

Fig.8 Variation of C_T, C_N, and C_M with H_2/H_1.

As is seen from Fig.8, with H_2/H_1 increasing, C_T rises, but C_N and C_M decline. This is because the top-wall pressure decreases with H_2/H_1 increasing, but the X-component of top-wall pressure increases, making both T and C_T increase; on the contrary, the Y-component decreases making both N and C_N decrease. The fact that enlarging H_2/H_1 would lower the top-wall pressure results in decrease in pitching moments. However, the influences H_2/H_1 exerts upon the pressure of internal nozzle are less significant than those upon the top-wall pressure of external nozzle, the pitching moment would decrease slightly because it is internal nozzle that produces the most part of pitching moment.

The calculated results show that when H_2/H_1 increases from 5 to 8, C_T rises by 10.8%, C_N and C_M reduce by 33.2% and 25.8% respectively. The sensibility coefficients, C_T, C_N, and C_M to H_2/H_1, which come in an escalating order, are equal to 0.18, 0.43 and 0.55.

3.4 Influences of cowl length L_s/H_1 upon nozzle performances

Fig.9 shows pressure contours with different L_s which are supposed to be $1.5H_1$, $4.5H_1$, $6.0H_1$ and $7.5H_1$ under the following condition: $L = 20H_1$, $\beta_B = 20°$, and $\theta = 0°$. From the figure, it is noted that the proportion of flow expansion in the internal nozzle increases gradually when L_s rises, but the exit pressure of internal nozzle decreases. Therefore, the rise of L_s results in the minus lift generated by internal cowl surfaces.

Fig.10 shows the variations of C_T, C_N, and C_M with L_s/H_1. The calculated results show that C_T increases slightly with L_s when $L_s/H_1 < 4.5$ with the

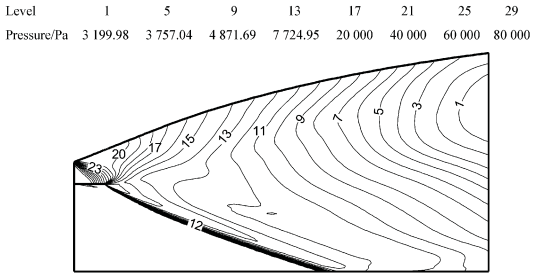

(a) $L_s = 1.5H_1$

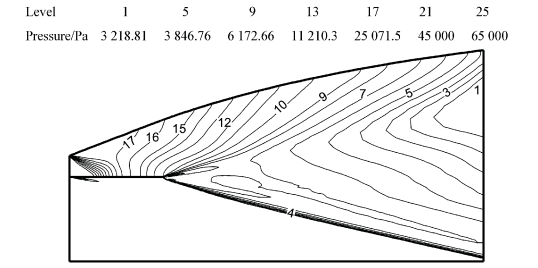

(b) $L_s = 4.5H_1$

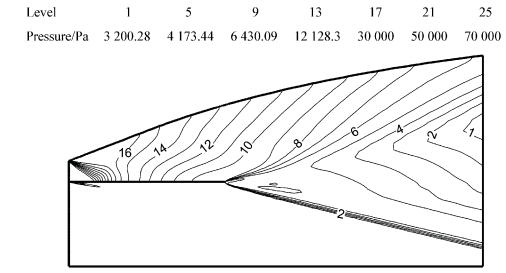

(c) $L_s = 6.0H_1$

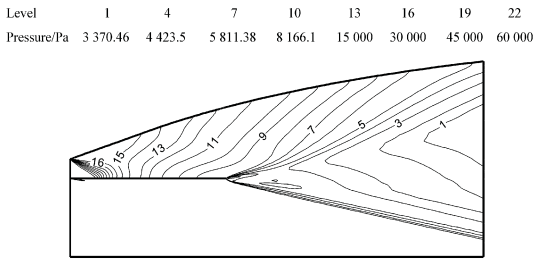

(d) $L_s = 7.5H_1$

Fig.9 Pressure contours with different L_s.

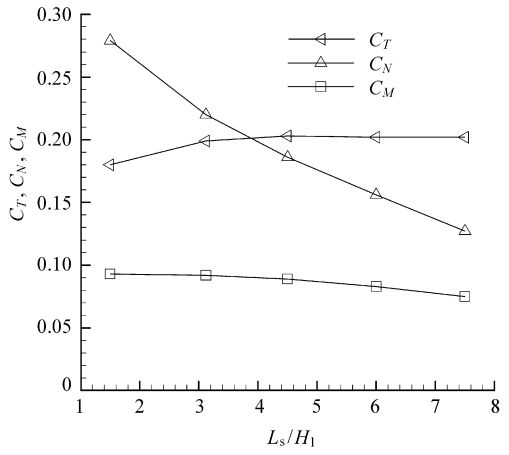

Fig.10 Variation of C_T, C_N, and C_M with L_s/H_1.

sensibility coefficient being 0.063, but once $L_s/H_1 > 4.5$, C_T stops changing. However, C_N decreases all the time when L_s increases. It stands to reason that with L_s rising, at the time that both up-wall pressure and lift increase, the higher minus lift is also generated by internal cowl surfaces. Therefore, the total lift drops sharply due to the joint effects of internal nozzle, which result in rapid decrease in lift coefficients. When L_s varies from $1.5H_1$ to $7.5H_1$, the sensibility coefficient of C_N is 0.273; and the minus lift increases with the rise of L_s, so the pitching moment coefficient decreases. When $1.5 < L_s/H_1 < 7.5$, the sensibility coefficient of C_M equals 0.061. As is discovered from Fig.10, the variation of C_N with L_s is the most remarkable of all sensibility coefficients with C_M coming the second.

3.5 Influences of cowl angle θ upon nozzle performances

Given $L = 20H_1$, $H_2/H_1 = 6$, $\beta_B = 20°$, $L_s = 3.12H_1$, and $\theta = 0°$, 3°, 6°, 9°, or 12°.

Fig.11 shows the variation of C_T, C_N, and C_M with θ. The calculated results show that, with the rise of θ, the nozzle up-wall thrust decreases and the cowl internal surface thrust increases with an almost constant thrust coefficient C_T, meaning the sensibility coefficient is almost zero. The up-wall lift decreases remarkably with θ rising. Therefore, both C_N and C_M present a downtrend with their sensibility coefficients being 0.15 and 0.24 respectively.

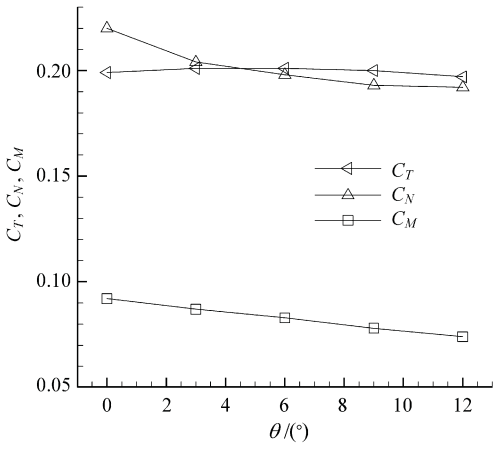

Fig.11 Variation of C_T, C_N, and C_M with θ.

Fig.12 shows the nozzle flow field pressure contours with different θ. It is noted that the single ramp expansion in nozzle entrance changes into a symmetry type when θ keeps rising. This implies that the flow expansion in the internal nozzle enlarges gradually and the nozzle exit pressure declines correspondingly.

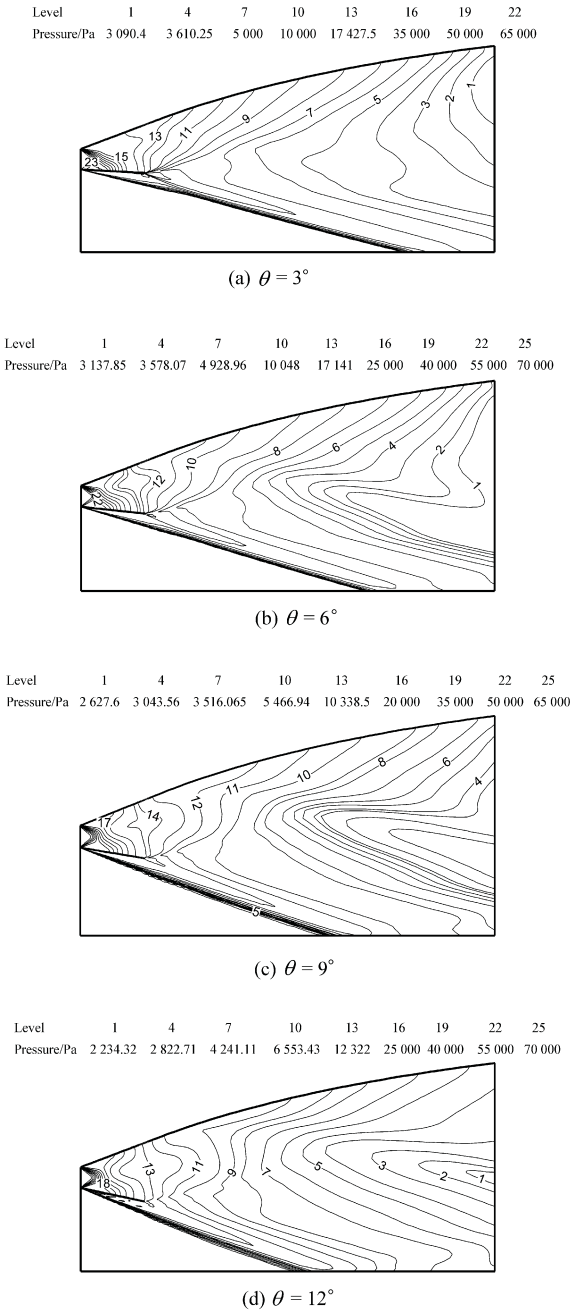

(a) $\theta = 3^\circ$

(b) $\theta = 6^\circ$

(c) $\theta = 9^\circ$

(d) $\theta = 12^\circ$

Fig.12 Pressure contours with different θ.

4 Conclusions

This article is intended to investigate the influences of geometric parameters upon scramjet nozzle performances by way of numerical simulation. The parameters under study include divergent angles, nozzle total lengths, height ratios, and cowl angles. The conclusions can be drawn as follows:

(1) C_T increases and C_N decreases as β_B increases with a slight alternation in C_M. In terms of sensibility to β_B, C_T, C_N, and C_M come in an escalating order.

(2) With the decrease of L, C_T suffers only a small amount of decrease, but C_N and C_M do a bigger one. The sensibility coefficients of C_T, C_N, and C_M to L with values of 0.12, 0.88 and 0.92 respectively change in an escalating order. On the premise of ensuring sufficient nozzle performances, a less total length is more preferable in designing practices.

(3) With increase in H_2/H_1, C_T rises due to sufficient expansion of external nozzle, but C_N and C_M decline. In terms of sensibility to H_2/H_1, C_T, C_N, and C_M come in an escalating order.

(4) C_N and C_M decrease with rise of L_s. C_N is the most remarkable of all sensibility coefficients to L_s with C_N coming second. When $L_s/H_1 < 4.5$, C_T increases slightly with L_s with the corresponding sensibility coefficient of 0.063, but once $L_s/H_1 > 4.5$, C_T stops changing.

(5) The sensibility coefficient of thrust coefficient C_T to θ is approximately zero. In contrast, both C_N and C_M present a downtrend with the corresponding sensibility coefficients being 0.15 and 0.24 respectively.

References

[1] Small W J, Weidner J P, Johnston P J. Scramjet nozzle design and analysis as applied to a highly integrated hypersonic research airplane. NASA TND-8334, 1976.

[2] Watanabe S. Scramjet nozzle experiment with hypersonic external flow. Journal of Propulsion and Power 1993; 9(4): 521-528.

[3] Saniovanni J J, Barber T J, Syed S A. Role of hydrogen/air chemistry in nozzle performance for hypersonic propulsion system. Journal of Propulsion and Power 1993; 9(1): 134-138.

[4] Starkey R P, Rankins F, Pins D. Coupled waverider/trajectory optimization for hypersonic cruise. AIAA-2005-530, 2005.

[5] Emanuel G. Gas dynamics theory and application. New York: AIAA Education Series, 1986.

[6] Lee S H, Mitani T. Reactive flow in scramjet external nozzle. AIAA-99-0616, 1999.

[7] Mitani T, Ueda S, Tani K, et al. Validation studies of scramjet nozzle performance. Journal of Propulsion and Power 1993; 9(5): 725-730.